The Conserved Salt Bridge in Human α-Defensin 5 Is Required for Its Precursor Processing and Proteolytic Stability*[S]◆

Mohsen Rajabi[‡], **Erik de Leeuw**[‡], **Marzena Pazgier**[§], **Jing Li**[‡], **Jacek Lubkowski**[§], and **Wuyuan Lu**[‡1]

From the [‡]Institute of Human Virology and Department of Biochemistry and Molecular Biology, University of Maryland School of Medicine, Baltimore, Maryland 21201 and the [§]Macromolecular Assembly Structure and Cell Signaling Section, NCI, National Institutes of Health, Frederick, Maryland 21702

Mammalian α-defensins, expressed primarily in leukocytes and epithelia, play important roles in innate and adaptive immune responses to microbial infection. Six invariant cysteine residues forming three indispensable disulfide bonds and one Gly residue required structurally for an atypical β-bulge are totally conserved in the otherwise diverse sequences of all known mammalian α-defensins. In addition, a pair of oppositely charged residues (Arg/Glu), forming a salt bridge across a protruding loop in the molecule, is highly conserved. To investigate the structural and functional roles of the conserved Arg^6–Glu^{14} salt bridge in human α-defensin 5 (HD5), we chemically prepared HD5 and its precursor proHD5 as well as their corresponding salt bridge-destabilizing analogs E14Q-HD5 and E57Q-proHD5. The Glu-to-Gln mutation, whereas significantly reducing the oxidative folding efficiency of HD5, had no effect on the folding of proHD5. Bovine trypsin productively and correctly processed proHD5 *in vitro* but spontaneously degraded E57Q-proHD5. Significantly, HD5 was resistant to trypsin treatment, whereas E14Q-HD5 was highly susceptible. Further, degradation of E14Q-HD5 by trypsin was initiated by the cleavage of the Arg^{13}–Gln^{14} peptide bond in the loop region, a catastrophic proteolytic event resulting directly in quick digestion of the whole defensin molecule. The E14Q mutation did not alter the bactericidal activity of HD5 against *Staphylococcus aureus* but substantially enhanced the killing of *Escherichia coli*. By contrast, proHD5 and E57Q-proHD5 were largely inactive against both strains at the concentrations tested. Our results confirm that the primary function of the conserved salt bridge in HD5 is to ensure correct processing of proHD5 and subsequent stabilization of mature α-defensin *in vivo*.

Defensins are expressed predominantly in leukocytes and epithelial cells as a family of cationic antimicrobial peptides that play important roles in innate and adaptive immune responses to microbial infection (1–5). In humans, defensins are classified into α- and β-families, differing by amino acid composition, cellular origin, and disulfide connectivity. To date, six human α-defensins have been identified, including four primarily from neutrophils, also known as human neutrophil peptides 1–4 or HNP1–4[2] (6–10) and two mainly from intestinal Paneth cells, also known as human defensins 5–6 or HD5–6 (11, 12). Although more than 30 putative β-defensin genes have been described using genomics tools (13–15), only a handful of β-defensins have been isolated and characterized at the protein level (16).

Human α-defensins are synthesized *in vivo* as significantly larger precursor molecules consisting of an N-terminal pro domain of 43–49 amino acid residues and a C-terminal Cys-rich defensin domain of 29–33 amino acid residues. The pro domain in proHNPs, important for correct folding, sorting, and trafficking of defensins (17–20), is proteolytically excised by yet-to-be-identified enzyme(s) prior to the storing of mature HNPs in the azurophilic granules of neutrophils. Immediately after phagocytosis, HNPs along with several antimicrobial enzymes including elastase are discharged into the microbe-containing phagocytic vacuole where microbial killing occurs (21). By contrast, stored in the granules of Paneth cells is unprocessed proHD5, which is secreted, both constitutively and inducibly, into the gut crypts of the small intestine where cleavages by trypsin generate mature HD5 (22).

A fully functional HD5 on the crypt and lumenal surfaces of intestinal epithelia is important for the innate defense against bacterial infection and may also provide antimicrobial protection for stem cells in the gut epithelial layer within the crypts (23). Bevins and colleagues (24) demonstrated in a mouse model that Paneth cells-associated expression of HD5 affords remarkable resistance of transgenic mice to oral challenge with virulent *Salmonella typhimurium*, providing support for a critical *in vivo* role of epithelial-derived defensins in mammalian host defense. Notably, the metalloproteinase matrilysin is required for the processing of mouse Paneth cell α-defensins (also known as cryptdins) (25). Mice deficient in matrilysin, thus lacking functional mature cryptdins, are highly suscep-

[2] The abbreviations used are: HNP, human neutrophil peptide; HD5, human α-defensin 5; HPLC, high pressure liquid chromatography; RP-HPLC, reverse phase-HPLC; ESI-MS, electrospray ionization-mass spectrometer; Boc, *t*-butoxycarbonyl.
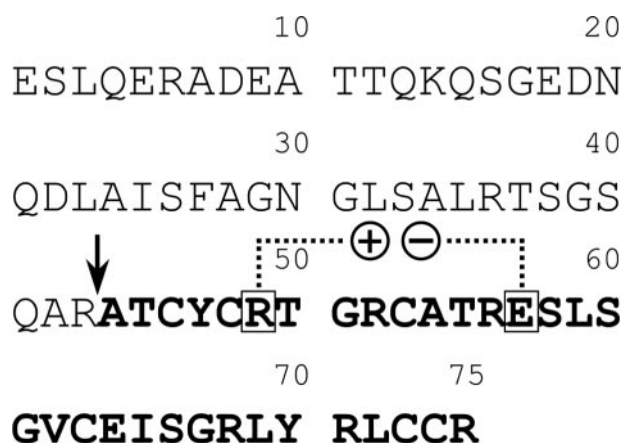
FIGURE 1. **The amino acid sequence of proHD5.** The mature domain is in *bold typeface,* and the maturation site is denoted by an *arrow.* The *boxed residues,* Arg[49] and Glu[57] in proHD5 or Arg[6] and Glu[14] in HD5, form a salt bridge in the structure and are highly conserved in all known mammalian α-defensins.

tible to orally administered *Salmonella,* indicative of the importance of cryptdins in defense against gut-associated pathogens (25, 26).

Sequence analysis of all known mammalian α-defensins indicates that in addition to the six Cys residues forming three structurally indispensable disulfide bridges and Gly[17], the salt bridge between Arg[5] and Glu[13] (HNP1 numbering) is highly conserved. Xie *et al.* (27) have previously shown that Gly[17] adopting unusual dihedral torsion angles is required for the formation of an atypical β-bulge structure conserved in the α-defensin family and that replacement of Gly[17] by any other ʟ-amino acids in HNP2 invariably results in defensin misfolding. In a separate study, Wu *et al.* (28) demonstrated that destabilization of the conserved Arg[5]–Glu[13] salt bridge in HNP1, whereas functionally inconsequential, dramatically accelerates proteolytic degradation of HNP1 by human neutrophil elastase, suggesting the importance of the salt bridge for defensin *in vivo* stability. Notably, Rosengren *et al.* (29) recently reported that destabilization of the conserved salt bridge in mouse cryptdin 4 (Crp4) through a series of mutations of Glu[15] (Crp4 numbering) has little impact on the bactericidal activity of the defensin, a result in agreement with that reported by Wu *et al.* (28). However, in contrast to the findings by Wu *et al.* (28), E15D-Crp4 and other salt bridge-deficient mutants are resistant to cleavage by the procryptdin processing enzyme matrilysin (29). The authors therefore concluded that the conserved salt bridge in Crp4 is not linked to proteolytic stability of the mature defensin (29).

To better understand why the salt bridge is conserved in α-defensins and to account for the reported discrepancy on its role in defensin stability, we expanded our study to include HD5 whose processing enzyme (trypsin) has been previously identified (22). We chemically synthesized HD5 and proHD5 as well as two corresponding salt bridge-destabilizing analogs: E14Q-HD5 and E57Q-proHD5 (Fig. 1). Detailed biochemical, functional, and structural characterizations of these synthetic defensin/pro defensin molecules help to establish that the conserved Arg[6]–Glu[14] (HD5 numbering) salt bridge is critical not only for correct processing of proHD5 by trypsin but also for

proteolytic stability of mature HD5 in the presence of its processing enzyme.

MATERIALS AND METHODS

Total Chemical Synthesis of HD5, proHD5, E14Q-HD5, and E57Q-proHD5—The amino acid sequences of HD5 and proHD5 are as follows: [1]ATCYC**R**TGRC[10]; [11]ATR**E**SLSGVC[20]; [21]EIS-GRLYRLC[30]; [31]CR (HD5); and [1]ESLQERADEA[10]; [11]TTQKQS-GEDN[20]; [21]QDLAISFAGN[30]; [31]GLSALRTSGS[40]; [41]QA**R**ATCY-C**R**T[50]; [51]GRCATR**E**SLS[60]; [61]GVCEISGRLY[70]; [71]RLCCR[75] (proHD5). Arg[43]–Ala[44] in proHD5 is the known processing site by trypsin both *in vivo* and *in vitro* (22). The conserved salt bridge is formed between Arg[6] and Glu[14] (in bold typeface) in HD5, as shown in the crystal structure of a chemically synthesized HD5 (30) (PDB code: 1zmp), and, presumably, between Arg[49] and Glu[57] in proHD5. Preparation of correctly folded synthetic HD5 used for this work was essentially as described previously (31). Similar procedures were used to synthesize E14Q-HD5. Native chemical ligation (32, 33) of the following peptide fragments was used to assemble proHD5 and E57Q-proHD5: (1–47)-proHD5-αCOSR (R = CH$_2$CH$_2$CO-Leu-OH), (5–32)-HD5, and E14Q-(5–32)-HD5. Syntheses of E14Q-HD5, (5–32)-HD5, and E14Q-(5–32)-HD5 on Boc-Arg(Tos)-OCH$_2$-PAM resin and of (1–47)-proHD5-αCOSR on Boc-Leu-OCH$_2$-PAM resin were performed using an in-house chemistry tailored from the *N,N*-diisopropylethylamine *in situ* neutralization/2-(1H-benzotriazolyl)-1,1,3,3-tetramethyluroniumhexafluorophosphate activation protocol originally developed by Kent and colleagues (34, 35) for Boc solid phase peptide synthesis. After chain assembly, the peptides were deprotected and cleaved by anhydrous hydrogen fluoride in the presence of 5% *p*-cresol at 0 °C for 1 h followed by precipitation with cold ether. All crude peptides were purified to homogeneity by preparative C18 reversed phase (RP) HPLC on a Waters Delta Prep 600 system, and their molecular masses were ascertained by a Micromass ZQ-4000 single quadrupole electrospray ionization-mass spectrometer (ESI-MS).

Native chemical ligation between (1–47)-proHD5-αCOSR and (5–32)-HD5 or E14Q-(5–32)-HD5 was carried out at a total peptide concentration of 13 mg/ml in 0.25 ᴍ phosphate buffer containing 6 ᴍ GuHCl and 2% (v/v) thiophenol, pH 7.5. The ligation reaction went to completion overnight at room temperature, yielding a full-length proHD5 or E57Q-proHD5, which was subsequently purified to homogeneity by preparative RP-HPLC. The determined molecular masses of fully reduced HD5, E14Q-HD5, proHD5, and E57Q-proHD5 were in agreement with the expected values calculated on the basis of the average isotopic compositions of the four synthetic molecules. All defensins were quantified by UV absorbance measurements at 280 nm using molar extinction coefficients calculated according to the algorithm published by Pace *et al.* (36).

Comparative Oxidative Folding of HD5, proHD5, E14Q-HD5, and E57Q-proHD5—Productive oxidative folding of HD5 was previously established (31). For comparison, reduced peptides were first dissolved at 2 mg/ml in 8 ᴍ urea containing 12 mᴍ reduced and 1.2 mᴍ oxidized glutathione followed by a 4-fold dilution with 0.25 ᴍ sodium bicarbonate. 30-µl aliquots were withdrawn at different time intervals (0, 0.5, 1, 2, 4, and 8 h), to

which an equal volume of 10% acetic acid was added to quench the reaction. The resultant solution (40 μl) was injected for HPLC analysis, which was performed at 40 °C on a Waters Symmetry™ C18 column (5 μm, 4.6 × 150 mm) using a linear gradient of 5–65% acetonitrile containing 0.1% trifluoroacetic acid at a flow rate of 1 ml/min over 30 min. For data points collected at time 0, a reducing buffer containing 0.25 M phosphate, 6 M GuHCl, and 0.01 mM dithiothreitol, pH 7.4, was used to dissolve peptide followed by acidification and HPLC quantification. The folding yields were calculated based on the ratio of the integrated areas of the two peaks given by folded defensin and fully reduced starting material.

Obtaining Correctly Folded E14Q-HD5 and R6A-HD5 from Pro Defensin—We also synthesized (R43M, E57Q)-proHD5 and (R43M, R49A)-proHD5 using native chemical ligation. The Met residue was introduced to facilitate chemical release of the C-terminal defensin domain after folding. The pro defensin mutant (R43M, E57Q)-proHD5 or (R43M, R49A)-proHD5 was folded in 2 M urea, 3 mM reduced glutathione, and 0.3 mM oxidized glutathione, pH 8.3. Quantitative cleavage of the Met[43]–Ala[44] peptide bond was achieved after an overnight reaction of the folded (R43M, E57Q)-proHD5 or (R43M, R49A)-proHD5 (1 mg/ml) with CNBr (25 mg/ml) in 2.5% trifluoroacetic acid, and the resultant E14Q-HD5 and R6A-HD5 were purified to homogeneity by RP-HPLC.

In Vitro Processing of proHD5 and E57Q-proHD5 by Trypsin—ProHD5 or E57Q-proHD5 at 0.5 mg/ml was incubated at room temperature with 0.01 mg/ml bovine trypsin (Worthington Biochemical Co.) in 50 mM Tris/HCl buffer containing 20 mM CaCl$_2$ and 0.001% Triton X-100, pH 8.3. Aliquots of 100 μl were withdrawn and quenched with 20 μl of 10% acetic acid at different time intervals (0.5, 1, 2, and 4 h), of which 60 μl was injected for RP-HPLC analysis on a Waters XBridge C18 column (3.5 μm, 4.6 × 150 mm) running a linear gradient of 5–45% acetonitrile containing 0.1% trifluoroacetic acid. ESI-MS was used to identify the cleavage products separated by analytical HPLC.

X-ray Crystallographic Studies of Trypsin-processed HD5—To verify the correct fold of the mature HD5 obtained by the processing of proHD5 with trypsin, we subjected it to the detailed crystallographic analysis. The crystallization and x-ray data collection protocols essentially replicated those described by us earlier for an HD5 preparation obtained by the folding of reduced defensin (30). The x-ray data collected for the single crystal of HD5 extended to the resolution of 2.1 Å. The space group (P6$_5$22) and unit cell parameters ($a = b = 49.52$ Å, $c = 254.9$ Å) were identical or nearly identical to reported previously (30). Using the program Phaser (37), the structure of HD5 could be easily solved with the model of this protein taken from the Protein Data base (Protein Data Bank entry code: 1zmp). A few steps of refinement with the program Refmac 5 (38), were sufficient to prove that the "new" structure of HD5 is virtually identical to previously reported. Values of the crystallographic R-factor and free-R for the final model were 0.217 and 0.258, respectively, and the root-mean-square deviation calculated for all the equivalent C$_\alpha$-atoms was less than 0.1 Å. The detail characteristics from the data collection and the structure refinement are shown in supplemental Table S1.

Proteolytic Stability of HD5 and E14Q-HD5—HD5 and E14Q-HD5 at 0.5 mg/ml each were incubated at room temperature with 0.0025 mg/ml bovine trypsin in 50 mM Tris/HCl buffer containing 20 mM CaCl$_2$ and 0.001% Triton X-100, pH 8.3. Aliquots of 80 μl were withdrawn at different time intervals (0, 0.5, 1, 2, 4, and 8 h for HD5; 0, 1, 5, 10, 15, 30, and 60 min for E14Q-HD5), acidified by 20 μl of 10% acetic acid, and injected (50 μl) for analysis on a Waters XBridge C18 column (3.5 μm, 4.6 × 150 mm) running a linear gradient of 5–45% acetonitrile containing 0.1% trifluoroacetic acid. The percentage of residual defensin was calculated based on the ratio of integrated peak areas of the intact molecule at a given time *versus* at time 0. The percentages of the intermediate produced due to the first cleavage at the Arg[13]–Gln[14] bond were calculated based on the ratio of integrated peak areas of cleaved E14Q-HD5 at a given time *versus* the intact starting material at time 0. Identical experiments were performed using R6A-HD5 and trypsin. In addition, the proteolytic stability of HD5 and E14Q-HD5 was examined under similar conditions with bovine chymotrypsin (Worthington Biochemical Co.), human leukocyte elastase (Elastin Products Co., Inc.), and human matrix metalloproteinase-7 (MMP-7) (Chemicon).

Antibacterial Activity of HD5, proHD5, E14Q-HD5, and E57Q-proHD5—Antimicrobial assays against *Escherichia coli* ATCC 25922 and *Staphylococcus aureus* ATCC 29213 (Microbiologics) were conducted using a previously detailed 96-well turbidimetric method dubbed virtual colony counting (39). A 2-fold dilution series of defensin, ranging from 25 to 0.098 μM in 10 mM sodium phosphate, pH 7.4, was incubated at 37 °C for 2 h with *E. coli* or *S. aureus* (1×10^6 colony-forming units/ml) followed by the addition of twice-concentrated Mueller-Hinton broth (2×) and 12-h kinetic measurements of bacterial growth at 650 nm.

RESULTS

The Arg[6]–Glu[14] Salt Bridge Is Important for In Vitro Oxidative Folding of HD5 but Dispensable for proHD5—We previously developed highly efficient protocols for *in vitro* oxidative folding of all six human α-defensins and some of their pro forms (20, 28, 31, 40, 41). As was demonstrated with HNP2, destabilization of the conserved salt bridge was detrimental to the folding of reduced HNP2 but had no adverse effect on the folding of reduced proHNP2 (28). To examine the role of the Arg[6]–Glu[14] salt bridge in the folding of HD5 and proHD5, we comparatively monitored time-dependent oxidative folding kinetics of HD5, E14Q-HD5, proHD5, and E57Q-proHD5 using analytical RP-HPLC coupled with ESI-MS, and the results are plotted in Fig. 2. Consistent with our previous finding that the pro peptide catalyzes oxidative folding of α-defensins *in vitro* (20), proHD5 folded significantly more efficiently than HD5, with nearly 90% of proHD5 folded within 2 h as opposed to ~40% of HD5 during the same time period. Although the yield of folded proHD5 plateaued at ~92% after 4 h, the yield of folded HD5 slowly increased over time to ~60% after 8 h.

Expectedly, destabilization of the salt bridge dramatically reduced the folding efficiency of HD5, as evidenced by merely a 5% yield of folded E14Q-HD5 during an 8-h time period. However, the folding kinetics of E57Q-proHD5 was nearly identical

to that of proHD5, suggesting that the salt bridge-destabilizing mutation (Glu[57] → Gln[57] in proHD5) had no impact on the folding of the defensin precursor. These results are entirely consistent with our previous findings on HNP2 (28). Shown in Fig. 3 are folded and purified proHD5 and E57Q-proHD5 on

FIGURE 2. **Time-dependent folding yields of HD5, proHD5, E14Q-HD5, and E57Q-proHD5.** Oxidative folding of each peptide was performed at a concentration of 0.5 mg/ml in 2 M urea, 3 mM reduced and 0.3 mM oxidized glutathione, pH 8.1. Samples were withdrawn at different time intervals for HPLC analysis. Yields, proportional to peak area, were calculated by integration. The data were obtained from two independent experiments, where the *error bars* represent the average deviation of the measurements.
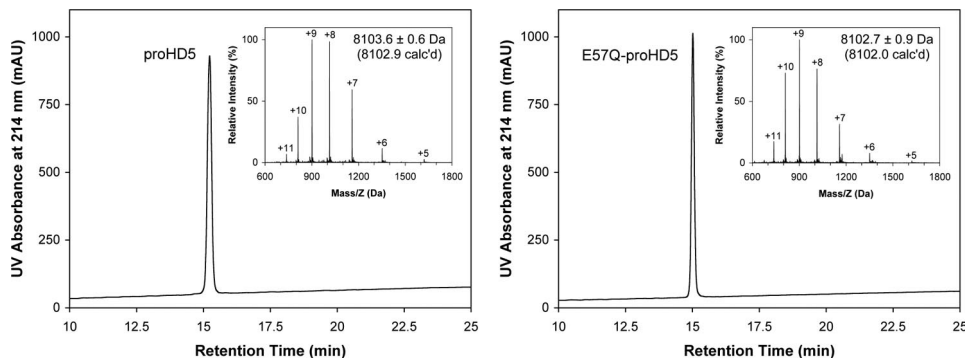
FIGURE 3. **Folded proHD5 and E57Q-proHD5 analyzed by RP-HPLC and ESI-MS.** HPLC analysis was performed at 40 °C on a Waters Symmetry™ 300 C18 column (5 μm, 4.6 × 150 mm) using a linear gradient of 5–65% acetonitrile containing 0.1% trifluoroacetic acid at a flow rate of 1 ml/min over 30 min. The measured molecular masses were in agreement with the expected values calculated based on the average isotopic compositions of the folded pro defensins. *mAU*, milliabsorbance units.

FIGURE 4. **Processing of proHD5 by trypsin at 30 min and 2 h.** HPLC analysis was performed at 40 °C on a Waters XBridge C18 column (3.5 μm, 4.6 × 150 mm) using a linear gradient of 5–45% acetonitrile containing 0.1% trifluoroacetic acid at a flow rate of 1 ml/min over 30 min. The chromatographic peaks were identified by ESI-MS analyses aided by simulated trypsin digestion. *mAU*, milliabsorbance units.

analytical RP-HPLC and ESI-MS. Their determined molecular masses of 8103.6 ± 0.6 and 8102.7 ± 0.9 Da are in good agreement with the expected values of 8102.9 and 8102.0 Da, respectively, calculated on the basis of average isotopic compositions of the folded pro defensins.

Trypsin Correctly and Efficiently Processes proHD5 in Vitro— Ghosh *et al.* (22) found that in human Paneth cells, trypsinogen is co-localized with proHD5 in the secretory granules. Upon secretion of proHD5 and trypsinogen, a yet-to-be-identified molecular event activates the enzyme, which in turn removes the pro region of proHD5, yielding predominantly mature HD5 and an N-terminally elongated (by an extra seven amino acid residues) minor processing product, i.e. [TSGSQAR]HD5 (22). To investigate the processing pathway of synthetic proHD5 *in vitro*, we incubated, at room temperature, 100 μg of proHD5 with 2 μg of bovine pancreatic trypsin in buffer, at pH 8.3, and monitored on HPLC and ESI-MS the cleavage reaction at different time intervals (30 min, 1 h, 2 h, and 4 h). The representative chromatographic traces collected at 30 min and 2 h are shown in Fig. 4. Within 30 min, proHD5 was nearly quantitatively converted to mature HD5 (found 3582.1 Da, expected 3582.2 Da), the minor processing product [TSGSQAR]HD5 (found 4269.9 Da, expected 4269.9 Da), and a major fragment from the pro peptide, 15–36 (found 2263.6 Da, expected 2263.4 Da). Over time, the extra seven amino acid residues at the N terminus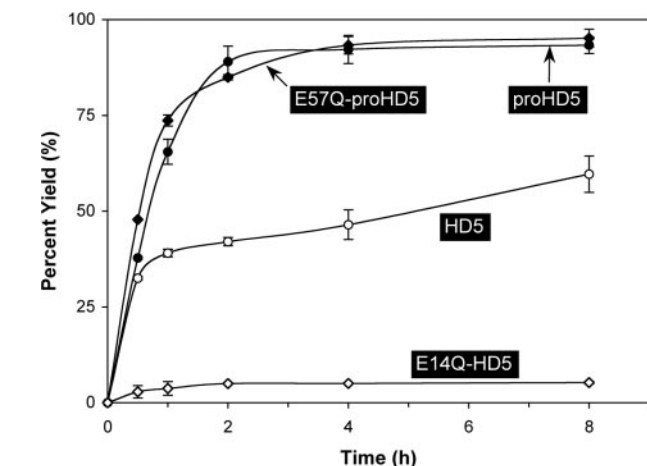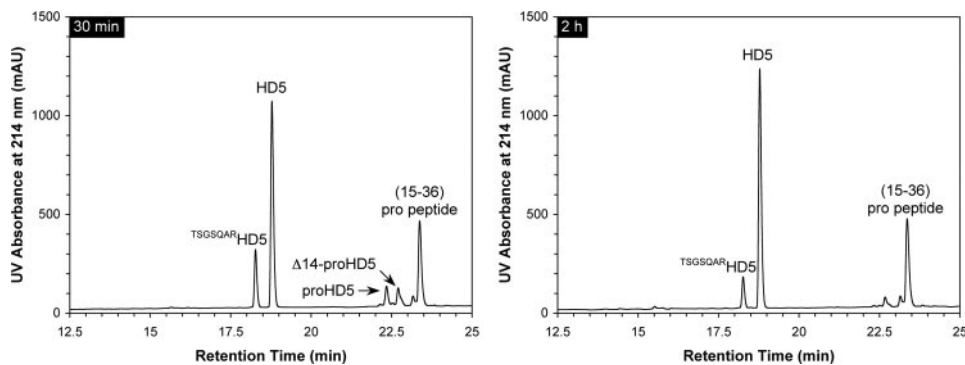 of [TSGSQAR]HD5 were slowly excised by trypsin, suggesting that the first and most productive cleavage in proHD5 occurs at the expected maturation site Arg[43]–Ala[44] rather than at the upstream site Arg[36]–Thr[37]. Notably, a transient, N-terminally truncated proHD5, Δ14-proHD5 (found 6515.7 Da, expected 6515.3 Da), was also detected during the cleavage reaction. Otherwise, intact HD5 largely remained as the terminally processed product during the entire time period (4 h).

Trypsin-processed HD5 Is Correctly Folded—We previously reported the crystal structure (1zmp) of a synthetic HD5 prepared by stepwise solid phase peptide synthesis (30). To demonstrate that oxidative folding of proHD5 and subsequent cleavage by trypsin yielded correctly folded HD5, we solved the crystal structure of trypsin-processed HD5 at 2.1 Å resolution. Shown in Fig. 5 are dimeric HD5 and its blown-up loop region stabilized by the Arg[6]–Glu[14] salt bridge, where two well defined H-bonds, at an average distance of 2.8 Å, are depicted between N[ε] and N[η2] of Arg[6] and O[ε1] and O[ε2] of Glu[14]. The charge-charge interaction, along
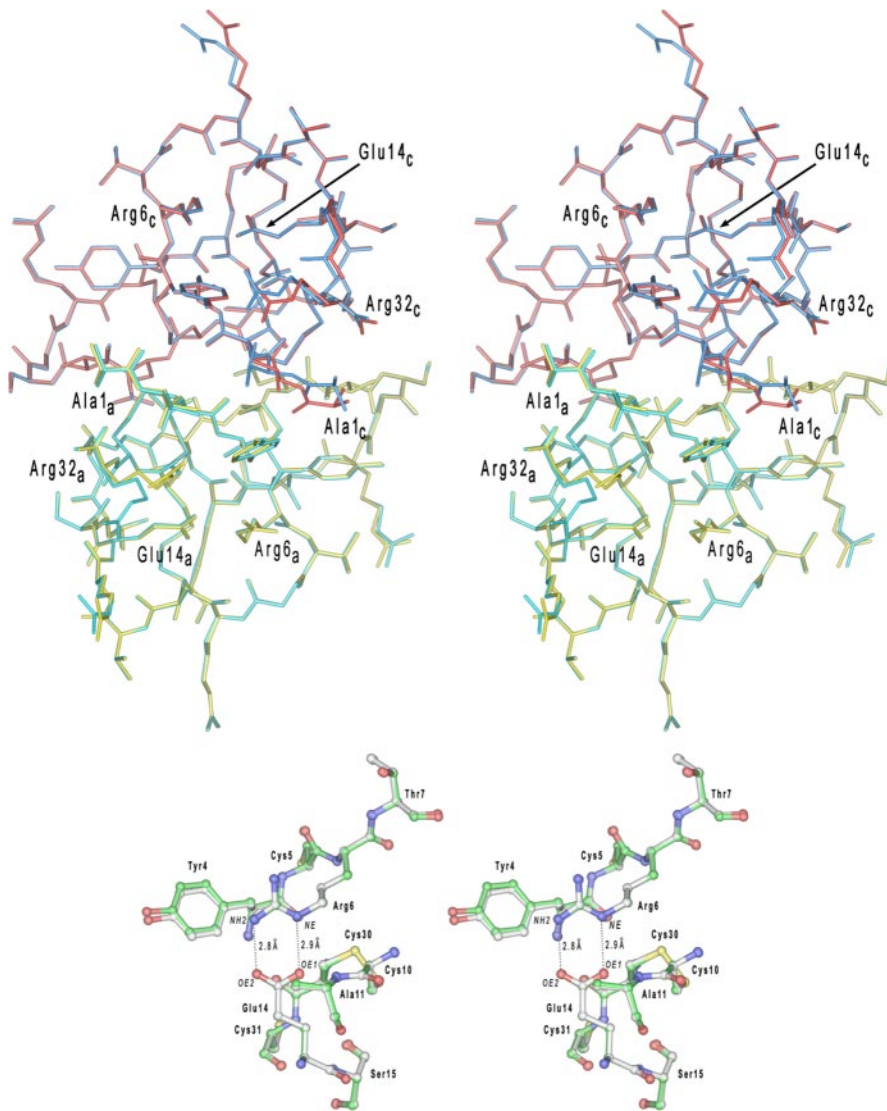
FIGURE 5. **Superposition of HD5 dimers in shown in a stereo representation.** In the *upper panel*, a dimer of HD5 colored in *yellow* and *red* represents the monomers A and C in the previously determined crystal structure of this defensin and deposited in the Protein Data Bank under the code 1zmp. The second dimer (colored in *cyan* and *blue*) is composed of monomers A and C from the current structure. The N- and C-terminal residues, as well as Arg[6] and Glu[14] (forming the salt bridge), are labeled for both monomers. Both structures are virtually indistinguishable (root mean square deviation for the 64 equivalent C_α-atoms is 0.088 Å) with slight deviations found only for few highly flexible side chains. A region of the Arg[6]–Glu[14] salt bridge is shown in the *lower panel* for both HD5 structures superimposed. The carbon atoms in the "1zmp" model are painted *white*, whereas in the current model, they are shown in *green*.
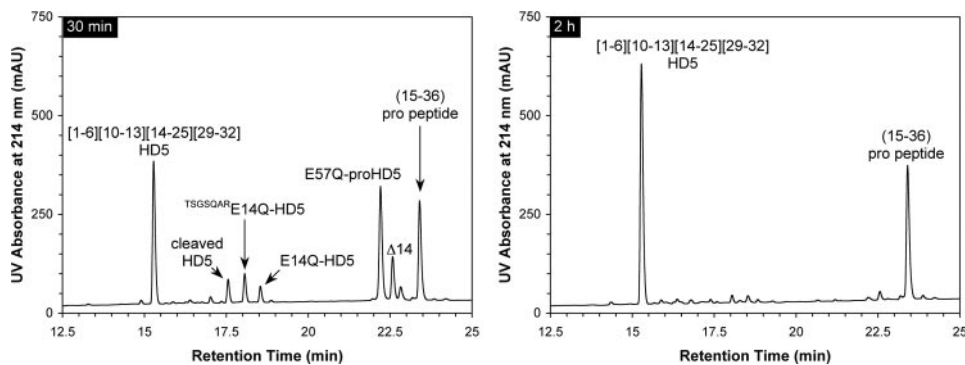

FIGURE 6. **Processing of E57Q-proHD5 by trypsin at 30 min and 2 h.** HPLC analysis was performed at 40 °C on a Waters XBridge C18 column (3.5 μm, 4.6 × 150 mm) using a linear gradient of 5–45% acetonitrile containing 0.1% trifluoroacetic acid at a flow rate of 1 ml/min over 30 min. The chromatographic peaks were identified by ESI-MS analyses aided by simulated trypsin digestion. *mAU*, milliabsorbance units.

with a perpendicular disulfide bond (Cys[10]–Cys[30]), stabilizes the extruding loop of HD5 encompassing Arg[6]-His[7]-Gly[8]-Arg[9]-Cys[10]-Ala[11]-Thr[12]-Arg[13]-Glu[14]. The overall structure of the trypsin-processed HD5 is virtually identical to the previously determined by us (Protein Data Bank code 1zmp). This result unambiguously shows that the folding and processing procedures utilized here lead to a correctly folded HD5.

Trypsin Processes E57Q-proHD5 but Spontaneously Degrades E57Q-proHD5—To investigate the effect of a destabilized salt bridge on the processing of the defensin precursor, we treated E57Q-proHD5 with trypsin the same way as described previously for wild type proHD5, and the chromatographic results obtained after 30 min and 2 h are illustrated in Fig. 6. Trypsin appeared to have correctly processed E57Q-proHD5, as evidenced by brief accumulation in the early stages of several similarly processed products seen in the processing of wild type proHD5, such as Δ14-E57Q-proHD5 (found 6514.3 Da, expected 6514.3 Da), E14Q-HD5 (found 3581.0 Da, expected 3581.2 Da), and ^{TSGSQAR}E14Q-HD5 (found 4269.2 Da, expected 4268.9 Da). However, E57Q-proHD5 was extremely prone to trypsin digestion. Within 30 min of incubation with trypsin, the majority of E57Q-proHD5 was converted to the terminal degradation product (1–6)(10–13)(14–25)(29–32), a fully cleaved defensin of four peptide fragments interconnected by three native disulfide bridges (Cys[1]–Cys[6], Cys[2]–Cys[4], and Cys[3]–Cys[5]) as judged by ESI-MS analyses (found 2889.3 Da, calculated 2889.4 Da). The major degradation product from the pro region, 15–36, in addition to several smaller peptide fragments that eluted early on RP-HPLC (not shown), also resulted. Within 2 h of incubation, E57Q-proHD5 was fully digested by trypsin to (1–6)(10–13)(14–25)(29–32), suggesting that destabilization of the conserved salt bridge is detrimental to proHD5
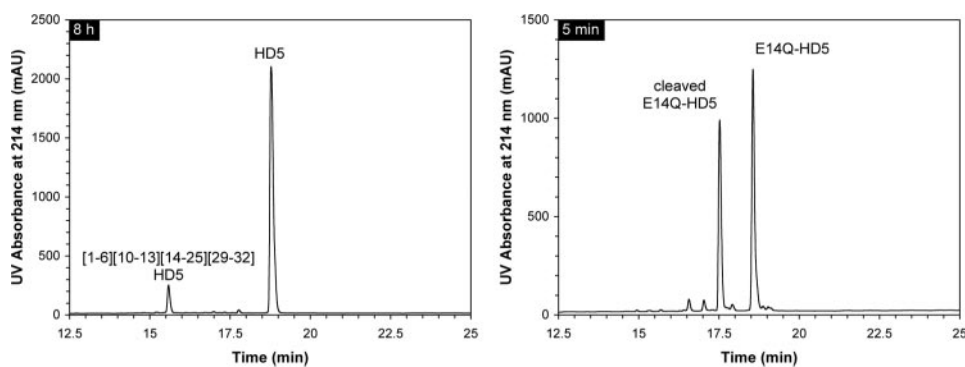
FIGURE 7. **Comparison of proteolytic susceptibility to trypsin between HD5 (8 h) and E14Q-HD5 (5 min).** HPLC analysis was performed at 40 °C on a Waters XBridge C18 column (3.5 μm, 4.6 × 150 mm) using a linear gradient of 5–45% acetonitrile containing 0.1% trifluoroacetic acid at a flow rate of 1 ml/min over 30 min. (1–6)(10–13)(14–25)(29–32)-HD5 is the terminal degradation product of HD5, whereas cleaved E14Q-HD5 represents the first intermediate with the internal Arg^{13}–Gln^{14} peptide bond hydrolyzed by trypsin. *mAU*, milliabsorbance units.
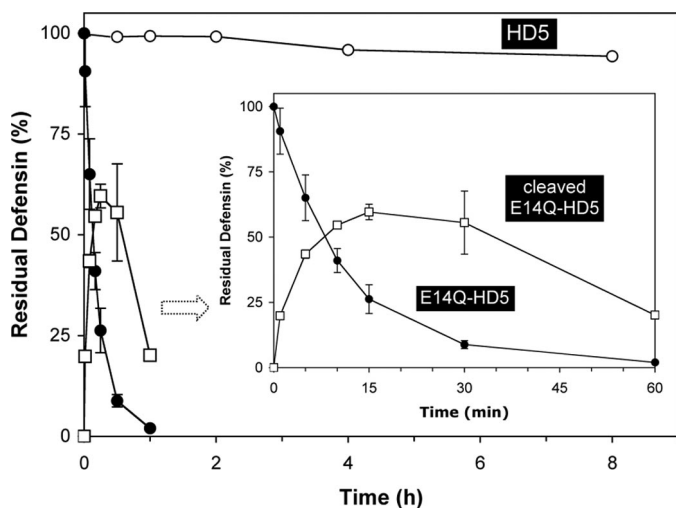

FIGURE 8. **Hydrolysis kinetics monitored for 8 h for HD5 and 60 min for E14Q-HD5 and cleaved E14Q-HD5.** Residual HD5 or E14Q-HD5 was calculated based on the ratio of integrated peak areas of the intact starting material at a given time *versus* at time 0. The percentage of cleaved E14Q-HD5 relative to the intact molecule was calculated in a similar fashion. The data were obtained from two independent experiments, where the *error bars* represent the average deviation of the measurements.

processing and that the C-terminal defensin domain confers proteolytic susceptibility of E57Q-proHD5.

Degradation of E14Q-HD5 by Trypsin Is Initiated by Cleavage of Arg^{13}–Gln^{14} in the Loop Region—To further examine the proteolytic susceptibility of E14Q-HD5 and to map out the sequence of events in its degradation by trypsin, we measured time-dependent hydrolysis kinetics of E14Q-HD5 on analytical RP-HPLC and ESI-MS, using a defensin-to-enzyme ratio of 200:1 (w/w). Wild type HD5 was used as a control. As shown in Figs. 7 and 8, wild type HD5 was resistant to trypsin treatment, with only 5% degraded to (^{1}ATCYCR^6)(^{10}CATR^{13})(^{14}ESLSGVCEISGR^{25})(^{29}LCCR^{32}) after 8 h (found 2890.5 Da; calculated 2890.4 Da). In sharp contrast, more than 35% of E14Q-HD5 was hydrolyzed within 5 min, 75% within 15 min, and over 98% within 60 min.

A careful examination of the cleavage of E14Q-HD5 by trypsin revealed that the first processing intermediate with only one internal cleavage in the sequence (found 3600.1 Da, expected 3600.2 Da; 18 mass units more than E14Q-HD5) eluted ~1 min

earlier on HPLC than E14Q-HD5 (Fig. 7). The same peak identified by ESI-MS also briefly appeared during the early stages of the processing of E57Q-proHD5 (Fig. 6). As intact E14Q-HD5 disappeared, the percentage of cleaved E14Q-HD5 increased (Fig. 8), reaching ~60% within 15 min, and then progressively decreased as smaller peptide fragments were generated. Reduction of cleaved E14Q-HD5 by dithiothreitol allowed us to identify two resultant peptide fragments on RP-HPLC whose molecular masses were found to be 1461.8 and 2143.3 Da, which corresponded to (1–13)-HD5 (calculated mass 1461.7 Da) and (14–32)-E14Q-HD5 (calculated mass 2143.5 Da), respectively. This result unequivocally demonstrated that degradation of E14Q-HD5 by trypsin was initiated by cleavage of Arg^{13}–Gln^{14} in the loop region, which propagated subsequent enzymatic cleavages at different Arg-Xaa sites throughout the molecule.

The salt bridge analog R6A-HD5 was also prone to degradation by trypsin (supplemental Fig. S1). Hydrolysis kinetics analysis indicated that the half-life of R6A-HD5 was ~30 min, and the enzyme digested more than 80% of the peptide within 4 h. Importantly, the first cleavage, as expected, occurred at the Arg^{13}–Glu^{14} site in the loop region. As compared with E14Q-HD5, however, R6A-HD5 was degraded less efficiently by trypsin, presumably due to a decreased number of trypsin cleavage sites in the molecule.

E14Q-HD5 Is Correctly Folded—We also attempted to determine the crystal structure of the E14Q-HD5 mutant. Small, irregularly shaped crystals were obtained. However, when subjected to the x-ray experiments, crystals displayed poor diffraction properties, and a very high mosaicity was evident. Consequently, we could not collect the diffraction data necessary for the detailed structural characterization of this mutant. To exclude the possibility that proteolytic susceptibility of E14Q-HD5 was attributable to defensin misfolding, we biochemically determined partial disulfide connectivity in its terminal degradation product, *i.e.* (^{1}ATCYCR^6)(^{10}CATR^{13})(^{14}QSLSGVCEISGR^{25})(^{29}LCCR^{32}). The terminally degraded product of E14Q-HD5 was further digested by chymotrypsin at room temperature in 50 mM Tris buffer containing 0.005% Triton X-100 and 20 mM CaCl$_2$, pH 8.3. The reaction was monitored by analytical RP-HPLC and ESI-MS. Chymotrypsin treatment yielded two major fragments on RP-HPLC, which were determined by ESI-MS to be (^{1}ATCY^4)(^{10}CATR^{13})(^{29}LCCR^{32}) (found 1395.3 Da, expected 1395.7 Da) and (^{5}CR^6)(^{17}SGVCEI^{22}) (found 881.6 Da, expected 882.0 Da). These results unambiguously demonstrated the presence of one native disulfide bond, Cys$^{5(2)}$–Cys$^{20(4)}$, and excluded the possibility of disulfide scrambling within the fragment containing, presumably, the remaining two disulfide bridges Cys$^{3(1)}$–Cys$^{31(6)}$ and Cys$^{10(3)}$–Cys$^{30(5)}$. Two additional pieces of evidence also supported correct folding of E14Q-HD5.
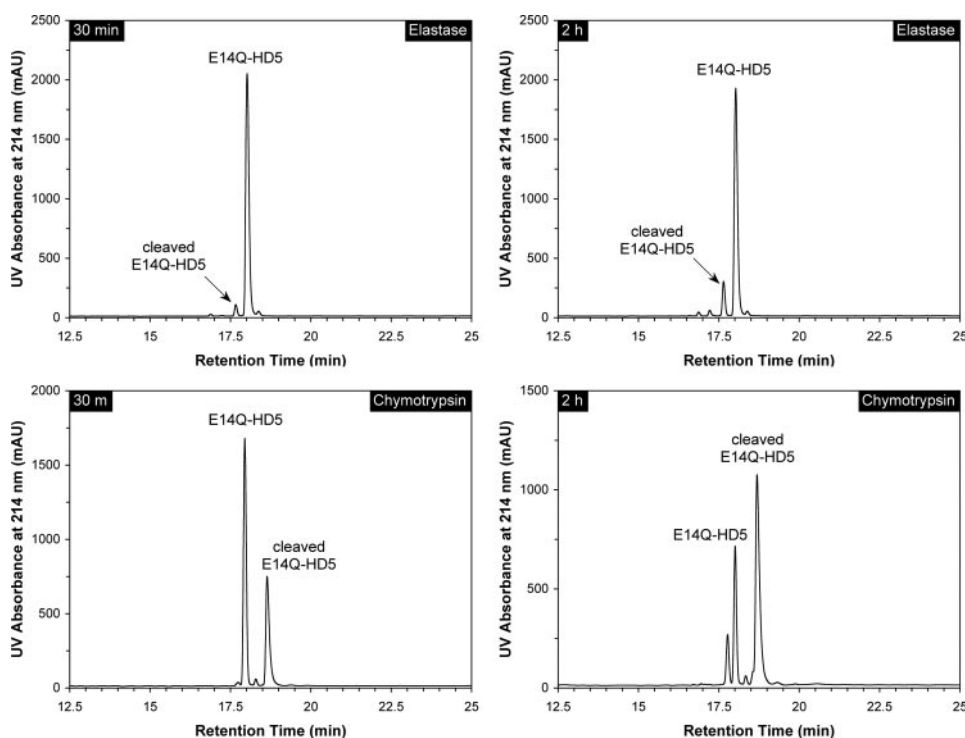
FIGURE 9. **Degradation of E14Q-HD5 by elastase and chymotrypsin at 30 min and 2 h.** Conditions for HPLC analysis were the same as described in the legends for Figs. 4, 6, and 7. For chymotrypsin, cleaved E14Q-HD5 differed from intact E14Q-HD5 by +18 Da in molecular mass, attributable to the cleavage of the Tyr[27]–Arg[28] peptide bond. The minor peak eluted before E14Q-HD5 after 2 h of incubation with the enzyme contained doubly and triply cleaved peptides as indicated by mass spectrometric analysis. *mAU*, milliabsorbance units.
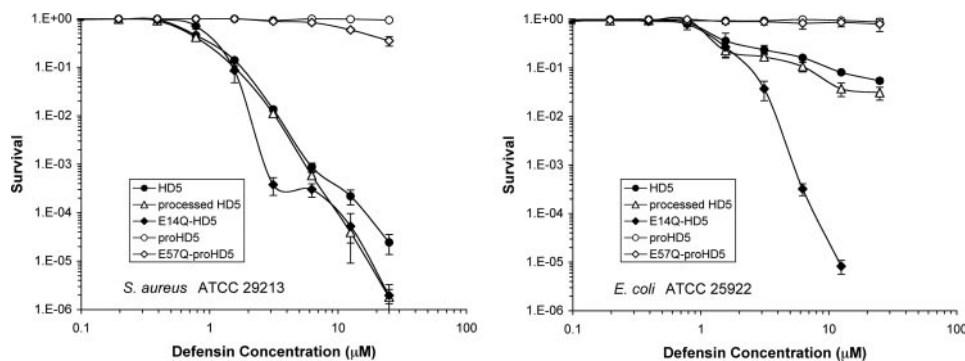

FIGURE 10. **Survival curves of *E. coli* ATCC 25299 (*left*) and *S. aureus* ATCC 29213 (*right*) exposed to HD5-derived peptides as indicated.** Strains were exposed to the peptides at concentrations varying 2-fold from 0.097 to 25 μM. Each curve is the mean of three separate experiments, where the *error bars* represent the standard deviation of the measurements. Points scored as zero survival could not be plotted.

First, the cleavage pattern from complete digestion of E14Q-HD5 by trypsin is entirely consistent with a native disulfide pairing in the mutant defensin. Second, it has been shown that the pro peptide of α-defensins intramolecularly chaperones correct folding of defensin precursors (20). When a defensin molecule contains mutations that incapacitate its ability to fold alone, covalent attachment of its pro peptide invariably rescues misfolding (28). For comparison, we prepared (R43M, E57Q)-proHD5 using native chemical ligation. CNBr cleavage of folded (R43M, E57Q)-proHD5 quantitatively released an E14Q-HD5 that was found identical to the separately folded E14Q-HD5 with respect to their chromatographic, mass spectrometric, and bactericidal properties as well as trypsin susceptibility (data not shown).

HD5 and E14Q-HD5 versus Other Proteases—Since chymotrypsin is present in the intestinal lumen under physiological conditions and elastase present during acute inflammation, we tested the proteolytic susceptibility of HD5 and E14Q-HD5 against bovine pancreatic chymotrypsin and human neutrophil elastase similarly to trypsin. For the wild type HD5, no detectable cleavage was observed within 4 h of incubation with either enzyme. E14Q-HD5 was relatively stable in the presence of elastase, with only 3% cleaved within 30 min, 13% within 2 h (Fig. 9), and one-third within 8 h. By contrast, E14Q-HD5 was much more susceptible to degradation by chymotrypsin. Within 30 min of incubation, 35% of the peptide was converted to an internally cleaved product (mass found 3600.2 Da), and the percentage increased to 65% within 2 h (Fig. 9). Unlike trypsin, chymotrypsin was inefficient in further processing its first cleavage product of E14Q-HD5. Disulfide reduction coupled with mass mapping unambiguously pinpointed the first chymotrypsin cleavage site to Tyr[27]–Arg[28] (found mass for fragment (1–27) 2955.5 Da, expected mass 2955.4 Da; found mass for fragment (28–32) 649.6 Da, expected mass 649.8 Da), consistent with chymotrypsin specificity. We also examined proteolytic susceptibility of HD5 and E14Q-HD5 to MMP-7 under identical conditions. However, no cleavage was detected on HPLC over a period of 8 h at room temperature.

The Functional Importance of the Conserved Salt Bridge in HD5 Appears Strain-specific—We tested the effect of the E14Q mutation in the salt bridge of HD5 on its antimicrobial activity against the Gram-negative bacterium *E. coli* and the Gram-positive bacterium *S. aureus* using virtual colony counting as established previously (39). In this assay, bacteria are exposed to a 2-fold serial dilution of peptides for 2 h. Subsequently, the antimicrobial activity of the peptides is neutralized by the addition of Mueller Hinton medium, and optical density is recorded for a period of 12 h as a measure for bacterial recovery. As shown in Fig. 10, HD5 effectively killed both strains of bacteria. Antimicrobial virtual lethal doses (in μM) that kill 50 and 90% of *E. coli* and *S. aureus* input viable cells, as inferred using the virtual colony counting procedure, are tabulated in supplemental Table S2. The virtual LD$_{50}$ and

virtual LD_{90} values of HD5 were comparable with the values reported previously for both strains tested (39). As expected, the antibacterial activity of HD5 derived from proHD5 via trypsin processing was virtually identical to that of a chemically synthesized HD5. Interestingly, although the bactericidal activity of E14Q-HD5 against *S. aureus* was comparable with that of the wild type peptide, E14Q-HD5 killed *E. coli* much more effectively at higher concentrations. At the highest peptide concentration tested (25 μM), *E. coli* did not recover after exposure to the E14Q-HD5 mutant peptide.

We also tested the effect of the pro domain on the antibacterial activities of these peptides. Only in the case of E57Q-proHD5, we observed modest killing of *S. aureus* at the two highest concentrations tested. Taken together, these data indicate that replacement of the glutamic acid in the conserved salt bridge of HD5 selectively alters the antibacterial properties of the peptide and that the pro domain acts to neutralize its bactericidal activity. Interestingly, a recombinant proHD5 was reported to be active against *S. typhymurium* and *Listeria monocytogenes* (22, 42). The disparity in antibacterial activity between recombinant and synthetic proHD5 may be attributable to the use of different test strains, assay conditions, and concentrations.

DISCUSSION

The Arg^6–Glu^{14} salt bridge found in HD5 is also highly conserved in other mammalian α-defensins except for guinea pig neutrophil α-defensins where the corresponding residues are Thr and Tyr (43). Wu *et al.* (28) reported that destabilization of the electrostatic interaction between Arg^5 and Glu^{13} in HNPs dramatically accelerated defensin *in vitro* degradation by elastase, one of several serine proteases co-localized with neutrophil α-defensins in the azurophilic granules, suggesting that the salt bridge in α-defensins is conserved for their *in vivo* stability. However, Rosengren *et al.* (29) recently showed that weakening of the corresponding Arg^7–Glu^{15} salt bridge in Crp4 by mutating Glu^{15} to Asp and several other amino acid residues had no effect on proteolytic susceptibility of the mouse α-defensin to its processing enzyme, matrilysin. It was therefore concluded that the salt bridge in mouse α-defensins is not conserved for their *in vivo* stability (29).

To help clarify the role of the conserved salt bridge in α-defensin structure and function, we chose human defensin 5 as a model compound because: 1) trypsin is known to be the processing enzyme of proHD5 *in vivo* and 2) trypsin readily recognizes the Arg-rich loop in HD5 (Arg^6-His^7-Gly^8-Arg^9-Cys^{10}-Ala^{11}-Thr^{12}-Arg^{13}-Glu^{14}) stabilized by the Arg^6–Glu^{14} salt bridge. We made the following findings. First, mutation of Glu^{14} to Gln significantly reduced oxidative folding efficiency of HD5 but had no effect on that of proHD5. Second, bovine trypsin productively and efficiently processed proHD5 *in vitro*, mimicking the activity of human trypsin *in vivo* (22), but spontaneously degraded E57Q-proHD5. Third, HD5 was resistant to trypsin treatment, whereas E14Q-HD5 was highly susceptible. Fourth, degradation of E14Q-HD5 by trypsin was initiated by the cleavage of the Arg^{13}–Gln^{14} peptide bond in the loop region. Finally, the E14Q mutation did not alter the bactericidal activity of HD5 against *S. aureus* but significantly enhanced the

killing of *E. coli*. By contrast, proHD5 and E57Q-proHD5 were largely inactive against both strains at the concentrations tested. Collectively, these results confirmed that the primary function of the conserved salt bridge in HD5 is to ensure correct processing of proHD5 and to stabilize the defensin *in vivo*.

How did Rosengren *et al.* (29) arrive at a conclusion totally different from ours then? The answer appears to lie in the choice of enzyme used in the susceptibility experiments. Although not the processing enzyme of human neutrophil α-defensin precursors, elastase preferably cleaves at multiple sites the extruding loop (Arg^5-Ile^6-Pro^7-Ala^8-Cys^9-Ile^{10}-Ala^{11}-Gly^{12}-Glu^{13}) stabilized by the Arg^5–Glu^{13} salt bridge in HNPs. By contrast, matrilysin, which prefers small hydrophilic residues at P1 and neutral residues at other subsite positions (44), is incapable of cleaving the heavily cationic loop in mouse cryptdin 4 (Arg^7-Lys^8-Gly^9-His^{10}-Cys^{11}-Lys^{12}-Arg^{13}-Gly^{14}-Glu^{15}) irrespective of the Arg^7–Glu^{15} salt bridge or lack thereof. As was demonstrated by this study using HD5 and HD5 analogs with trypsin, chymotrypsin, elastase, and matrilysin, the outcome is entirely dependent on the choice of enzyme used. Despite its physiological relevance to the processing of pro cryptdins *in vivo*, matrilysin, lacking the specificity to cleave the loop region, appears in retrospect to be an inappropriate choice of enzyme for the question of why the Arg^7–Glu^{15} salt bridge is conserved in mouse cryptdins. Of note, it was recently brought to our attention that trypsin has been used to test proteolytic susceptibility of Crp4 and a series of its salt bridge destabilizing mutants, and the Arg^7–Glu^{15} salt bridge was indeed found critical for proteolytic stability of the mouse α-defensin, in agreement with our current and earlier reports.[3]

α-Defensins, due to their small size, lack sufficient hydrophobic packing and are structurally stabilized by the three disulfide bridges Cys^1–Cys^6, Cys^2–Cys^4, and Cys^3–Cys^5 (sequential numbering). The extruding loop connecting the first and second β-strands presents the third Cys residue for disulfide bonding and is stabilized by the conserved Arg^6–Glu^{14} salt bridge perpendicular to Cys^3–Cys^5 (Fig. 5). Mutation of Glu^{14} to Gln^{14} in HD5 dramatically reduced defensin folding efficiency, suggesting the importance of the salt bridge in stabilizing the loop to orient Cys^3 for correct disulfide pairings, although loss of such stabilization is well tolerated in the folding of proHD5, where the pro peptide itself can catalyze pro defensin folding through favorable intramolecular interactions (20). It becomes apparent that the β-strand-connecting loop, present in all known mammalian α-defensins, is structurally indispensable for the correct α-defensin fold.

Proteases cleave protein substrates preferably in loops. The reason is 2-fold. First, loops, unlike ordered secondary structures such as α-helices and β-strands, can readily insert into the S1 specificity pocket of the enzyme with minimal steric hindrance. Second, loops are in general flexible, assuming a low free energy barrier to the transition state of the productive enzyme-substrate complex. Thus, conformational rigidity in the loop region of a protein is critical for "slowing down" otherwise efficient proteolytic cleavage (45). Understandably, fur-

---

ther hydrolysis of HD5 in the presence of its processing enzyme trypsin was extremely slow due to loop stabilization afforded by the conserved salt bridge. By contrast, destabilization of the salt bridge in HD5 lessened the rigidity of the loop, rendering the loop susceptible to trypsin hydrolysis. The first cleavage by trypsin between Arg[13] and Gln[14] in the loop of E14Q-HD5 led to global destabilization of the defensin molecule presumably due to the loss of structural support to the Cys[3]–Cys[5] disulfide and to weakened inter-β-strand interactions as well. Consequently, a dramatic acceleration of hydrolysis ensued. Notably, loss of the salt bridge in E14Q-HD5 perpetuated chymotrypsin cleave of Tyr[27]–Arg[28], a site distal to the loop region, further demonstrating a propagated global effect of local structural destabilization on the proteolytic susceptibility of α-defensins.

Mutation of Glu[14] to Gln[14] in HD5 potentially creates a trypsin cleavage site at the Arg[6]–Thr[7] peptide bond. In the NMR structure of E15D-Crp4, the side chain of Arg[7] rotates out and projects into the solution, making itself accessible to the recognition by trypsin (29). Although it is tempting to suggest that a freed Arg[6] in E14Q-HD5 directly contributes to defensin degradation, our findings on the initiation of trypsin cleavage indicate otherwise. Trypsin cleavage of E14Q-HD5 did not appear to be a random proteolytic event. Rather, it was specifically linked to loss of the salt bridge, thus destabilization of the protruding loop structure in the molecule. The results on R6A-HD5 clearly supported this conclusion.

Cationic charges functionally contribute to microbial killing by defensins (46–49). Mutation of Glu[14] to Gln[14] in the salt bridge frees up Arg[6], thus increasing the cationicity of HD5. It is therefore reasonable to expect an enhanced bactericidal activity from E14Q-HD5 as compared with wild type HD5. This was clearly the case with *E. coli*. However, the Glu[14]-to-Gln[14] mutation did not affect the killing of *S. aureus*. Interestingly, breakage of the salt bridge in HNP2 had little effect on the killing of either *E. coli* or *S. aureus* (28). Similar results were also reported for salt bridge-deficient mutants of mouse cryptdin 4 (29), which, as compared with the wild type Crp4, showed little difference in their bactericidal activity against multiple strains. Thus, it appears that the functional ramification of neutralization of the anionic partner in the conserved salt bridge is dependent not only on bacterial strains but also on defensin species. These findings are not entirely surprising in light of the previous reports that bacterial killing by defensins is in general strain- and sequence-specific (39), although the molecular determinants for defensin activity and specificity still remain poorly defined. It is worth pointing out that *S. aureus* killing by HD5 is structure (disulfide)-dependent, whereas *E. coli* killing by HD5 is not (50). In contrast, killing of both *E. coli* and *S. aureus* by human β-defensin 3 is structure (disulfide)-independent (51–53). Functional disparities seen in the action of a variety of defensins may be a reflection of molecular complexity involving defensin interactions with not just the bacterial membrane but with diverse bacterial cell wall components as well.

REFERENCES

1. Ganz, T. (2003) *Nat. Immunol.* **3,** 710–720
2. Lehrer, R. I. (2004) *Nat. Rev. Microbiol.* **2,** 727–738
3. Selsted, M. E., and Ouellette, A. J. (2005) *Nat. Immunol.* **6,** 551–557
4. Zasloff, M. (2002) *Nature* **415,** 389–395
5. Yang, D., Biragyn, A., Hoover, D. M., Lubkowski, J., and Oppenheim, J. J. (2004) *Annu. Rev. Immunol.* **22,** 181–215
6. Selsted, M. E., Harwig, S. S., Ganz, T., Schilling, J. W., and Lehrer, R. I. (1985) *J. Clin. Investig.* **76,** 1436–1439
7. Ganz, T., Selsted, M. E., Szklarek, D., Harwig, S. S., Daher, K., Bainton, D. F., and Lehrer, R. I. (1985) *J. Clin. Investig.* **76,** 1427–1435
8. Gabay, J. E., Scott, R. W., Campanelli, D., Griffith, J., Wilde, C., Marra, M. N., Seeger, M., and Nathan, C. F. (1989) *Proc. Natl. Acad. Sci. U. S. A.* **86,** 5610–5614
9. Wilde, C. G., Griffith, J. E., Marra, M. N., Snable, J. L., and Scott, R. W. (1989) *J. Biol. Chem.* **264,** 11200–11203
10. Singh, A., Bateman, A., Zhu, Q. Z., Shimasaki, S., Esch, F., and Solomon, S. (1988) *Biochem. Biophys. Res. Commun.* **155,** 524–529
11. Jones, D. E., and Bevins, C. L. (1992) *The J. Biol. Chem.* **267,** 23216–23225
12. Jones, D. E., and Bevins, C. L. (1993) *FEBS Lett.* **315,** 187–192
13. Jia, H. P., Schutte, B. C., Schudy, A., Linzmeier, R., Guthmiller, J. M., Johnson, G. K., Tack, B. F., Mitros, J. P., Rosenthal, A., Ganz, T., and McCray, P. B., Jr. (2001) *Gene (Amst.)* **263,** 211–218
14. Schutte, B. C., Mitros, J. P., Bartlett, J. A., Walters, J. D., Jia, H. P., Welsh, M. J., Casavant, T. L., and McCray, P. B., Jr. (2002) *Proc. Natl. Acad. Sci. U. S. A.* **99,** 2129–2133
15. Dorin, J. R., and Jackson, I. J. (2007) *Science* **318,** 1395
16. Pazgier, M., Hoover, D. M., Yang, D., Lu, W., and Lubkowski, J. (2006) *CMLS Cell Mol. Life Sci.* **63,** 1294–1313
17. Liu, L., and Ganz, T. (1995) *Blood* **85,** 1095–1103
18. Valore, E. V., Martin, E., Harwig, S. S., and Ganz, T. (1996) *J. Clin. Investig.* **97,** 1624–1629
19. Valore, E. V., and Ganz, T. (1992) *Blood* **79,** 1538–1544
20. Wu, Z., Li, X., Ericksen, B., de Leeuw, E., Zou, G., Zeng, P., Xie, C., Li, C., Lubkowski, J., Lu, W. Y., and Lu, W. (2007) *J. Mol. Biol.* **368,** 537–549
21. Segal, A. W. (2005) *Annu. Rev. Immunol.* **23,** 197–223
22. Ghosh, D., Porter, E., Shen, B., Lee, S. K., Wilk, D., Drazba, J., Yadav, S. P., Crabb, J. W., Ganz, T., and Bevins, C. L. (2002) *Nat. Immunol.* **3,** 583–590
23. Zasloff, M. (2002) *Nat. Immunol.* **3,** 508–510
24. Salzman, N. H., Ghosh, D., Huttner, K. M., Paterson, Y., and Bevins, C. L. (2003) *Nature* **422,** 522–526
25. Wilson, C. L., Ouellette, A. J., Satchell, D. P., Ayabe, T., Lopez-Boado, Y. S., Stratman, J. L., Hultgren, S. J., Matrisian, L. M., and Parks, W. C. (1999) *Science* **286,** 113–117
26. Ouellette, A. J. (2006) *Curr. Top. Microbiol. Immunol.* **306,** 1–25
27. Xie, C., Prahl, A., Ericksen, B., Wu, Z., Zeng, P., Li, X., Lu, W. Y., Lubkowski, J., and Lu, W. (2005) *J. Biol. Chem.* **280,** 32921–32929
28. Wu, Z., Li, X., de Leeuw, E., Ericksen, B., and Lu, W. (2005) *J. Biol. Chem.* **280,** 43039–43047
29. Rosengren, K. J., Daly, N. L., Fornander, L. M., Jonsson, L. M., Shirafuji, Y., Qu, X., Vogel, H. J., Ouellette, A. J., and Craik, D. J. (2006) *J. Biol. Chem.* **281,** 28068–28078
30. Szyk, A., Wu, Z., Tucker, K., Yang, D., Lu, W., and Lubkowski, J. (2006) *Protein Sci.* **15,** 2749–2760
31. Wu, Z., Ericksen, B., Tucker, K., Lubkowski, J., and Lu, W. (2004) *J. Pept. Res.* **64,** 118–125
32. Dawson, P. E., and Kent, S. B. (2000) *Annu. Rev. Biochem.* **69,** 923–960
33. Dawson, P. E., Muir, T. W., Clark-Lewis, I., and Kent, S. B. (1994) *Science* **266,** 776–779
34. Schnolzer, M., Alewood, P., Jones, A., Alewood, D., and Kent, S. B. (1992) *Int. J. Pept. Protein Res.* **40,** 180–193
35. Kent, S. B. (1988) *Annu. Rev. Biochem.* **57,** 957–989
36. Pace, C. N., Vajdos, F., Fee, L., Grimsley, G., and Gray, T. (1995) *Protein Sci.* **4,** 2411–2423
37. Read, R. J. (2001) *Acta Crystallogr. Sect. D Biol. Crystallogr.* **57,** 1373–1382
38. Murshudov, G. N., Vagin, A. A., Lebedev, A., Wilson, K. S., and Dodson, E. J. (1999) *Acta Crystallogr. Sect. D Biol. Crystallogr.* **55,** 247–255

39. Ericksen, B., Wu, Z., Lu, W., and Lehrer, R. I. (2005) *Antimicrob. Agents Chemother.* **49,** 269–275

40. Wu, Z., Powell, R., and Lu, W. (2003) *J. Am. Chem. Soc.* **125,** 2402–2403

41. Wu, Z., Prahl, A., Powell, R., Ericksen, B., Lubkowski, J., and Lu, W. (2003) *J. Pept. Res.* **62,** 53–62

42. Tanabe, H., Ayabe, T., Maemoto, A., Ishikawa, C., Inaba, Y., Sato, R., Moriichi, K., Okamoto, K., Watari, J., Kono, T., Ashida, T., and Kohgo, Y. (2007) *Biochem. Biophys. Res. Commun.* **358,** 349–355

43. Selsted, M. E., and Harwig, S. S. (1987) *Infect Immun.* **55,** 2281–2286

44. Turk, B. E., Huang, L. L., Piro, E. T., and Cantley, L. C. (2001) *Nat. Biotechnol.* **19,** 661–667

45. Lu, W. Y., Starovasnik, M. A., Dwyer, J. J., Kossiakoff, A. A., Kent, S. B., and Lu, W. (2000) *Biochemistry* **39,** 3575–3584

46. Satchell, D. P., Sheynis, T., Kolusheva, S., Cummings, J., Vanderlick, T. K., Jelinek, R., Selsted, M. E., and Ouellette, A. J. (2003) *Peptides* **24,** 1795–1805

47. Tanabe, H., Qu, X., Weeks, C. S., Cummings, J. E., Kolusheva, S., Walsh, K. B., Jelinek, R., Vanderlick, T. K., Selsted, M. E., and Ouellette, A. J. (2004) *J. Biol. Chem.* **279,** 11976–11983

48. Hancock, R. E. (1997) *Lancet* **349,** 418–422

49. Zou, G., de Leeuw, E., Li, C., Pazgier, M., Zeng, P., Lu, W. Y., Lubkowski, J., and Lu, W. (2007) *J. Biol. Chem.* **282,** 19653–19665

50. de Leeuw, E., Burks, S. R., Li, X., Kao, J. P., and Lu, W. (2007) *FEBS Lett.* **581,** 515–520

51. Kluver, E., Schulz-Maronde, S., Scheid, S., Meyer, B., Forssmann, W. G., and Adermann, K. (2005) *Biochemistry* **44,** 9804–9816

52. Taylor, K., Clarke, D. J., McCullough, B., Chin, W., Seo, E., Yang, D., Oppenheim, J., Uhrin, D., Govan, J. R., Campopiano, D. J., Macmillan, D., Barran, P. E., and Dorin, J. R. (2008) *J. Biol. Chem.* **283,** 6631–6639

53. Wu, Z., Hoover, D. M., Yang, D., Boulegue, C., Santamaria, F., Oppenheim, J. J., Lubkowski, J., and Lu, W. (2003) *Proc. Natl. Acad. Sci. U. S. A.* **100,** 8880–8885